Supporting Information

Carrier Transport Engineering in Carbon Nanotubes by Chirality Induced Spin Polarization

Md. Wazedur Rahman[1], Seyedamin Firouzeh[1], Vladimiro Mujica[2], Sandipan Pramanik[1,*]

[1]Department of Electrical and Computer Engineering, University of Alberta, Edmonton, AB T6G 2V4, Canada

[2]School of Molecular Sciences, Box 871604, Arizona State University, Tempe, AZ 85287-1604, USA

[*]Corresponding Author (spramani@ualberta.ca)

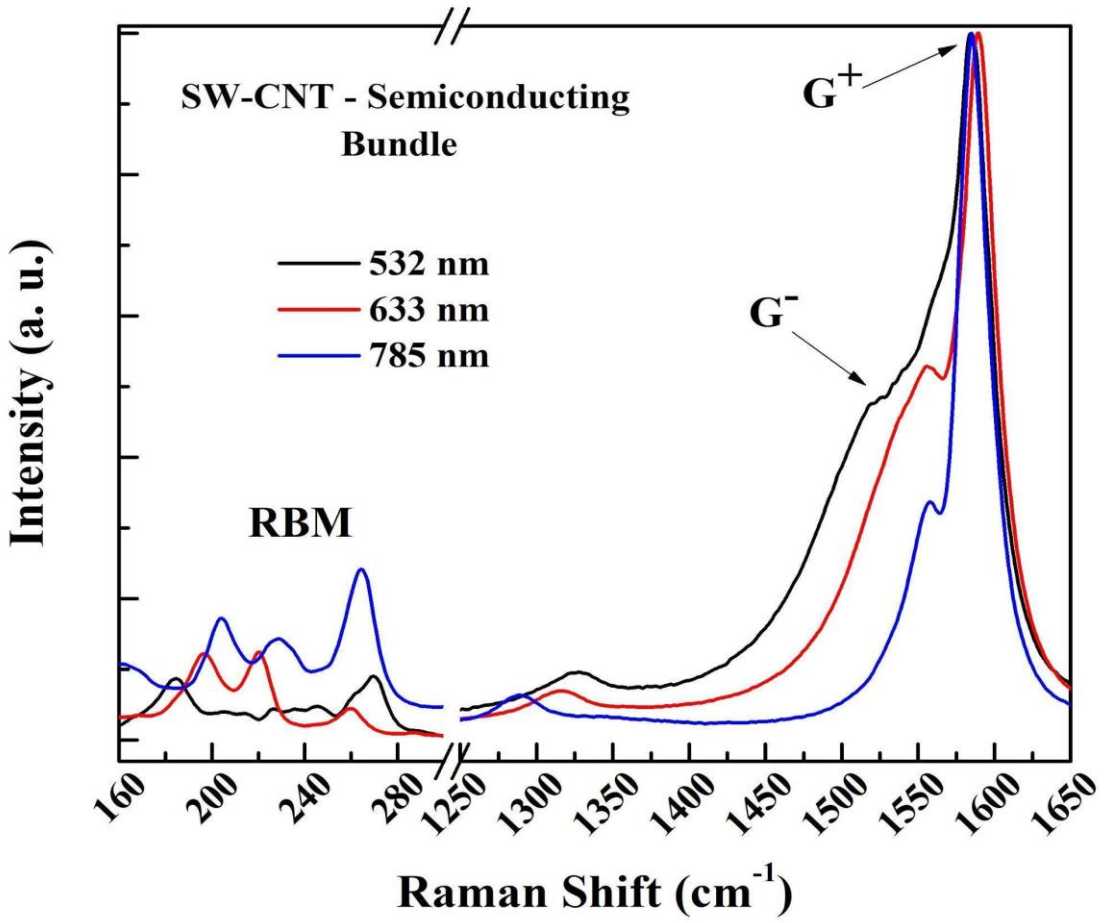

Figure S1. Raman characterizations carried out at multiple laser frequencies on as-purchased bundled nanotubes. No Breit-Wigner-Fano (B-W-F) lineshape has been observed at any frequency, indicating that the nanotubes are predominantly semiconducting. Defect peak (~ 1340 cm^{-1}) is negligible for bundled specimens.

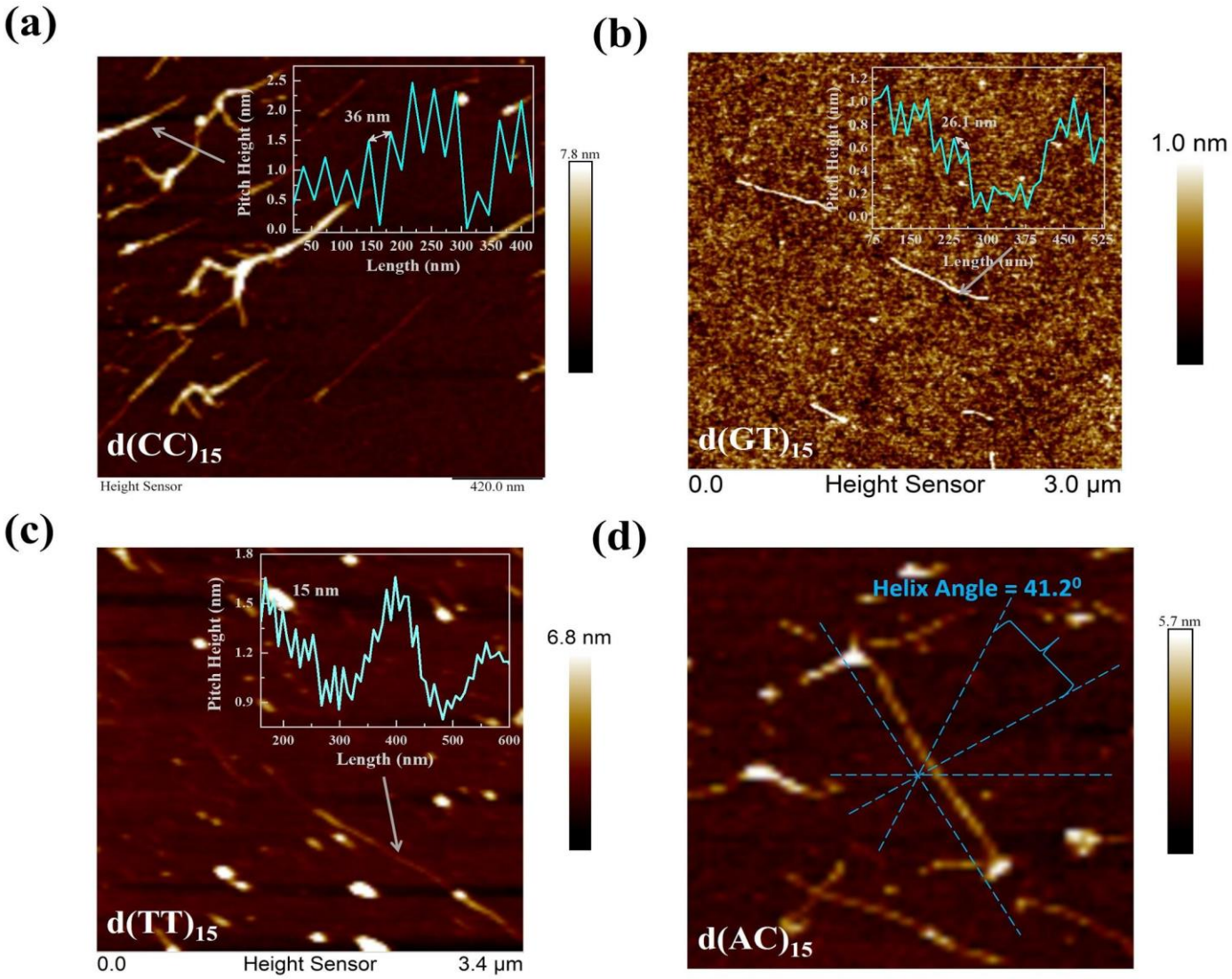

Figure S2. Typical AFM images of (a) $d(CC)_{15}$, (b) $d(GT)_{15}$ and (c) $d(TT)_{15}$ wrapped nanotubes dispersed on SiO_2 substrate. *Insets* show line scan along nanotube lengths. Alternating bands of high and low regions are observed indicating helical wrapping. (d) Estimation of helix tilt angle from Fig. 1(a) in the main paper.

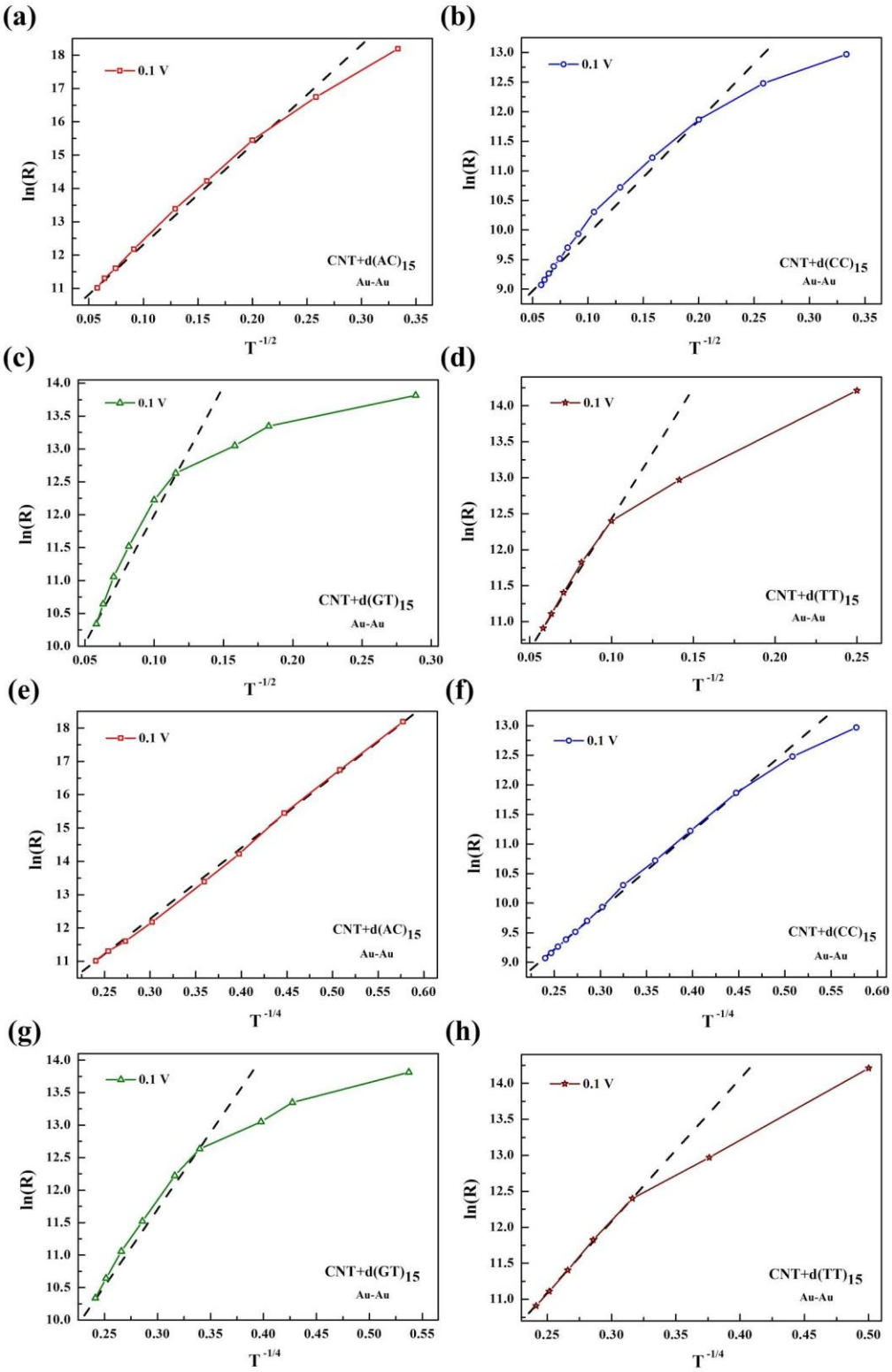

Figure S3. ln R vs. $(1/T)^{(1/(d+1))}$ plots (VRH model) for (a)-(d) d = 1 and (e)-(h) d = 3. $d(AC)_{15}$ and $d(CC)_{15}$ functionalized samples show small deviations at low temperatures, whereas for $d(GT)_{15}$ and $d(TT)_{15}$ functionalizations, the deviation is significantly larger.

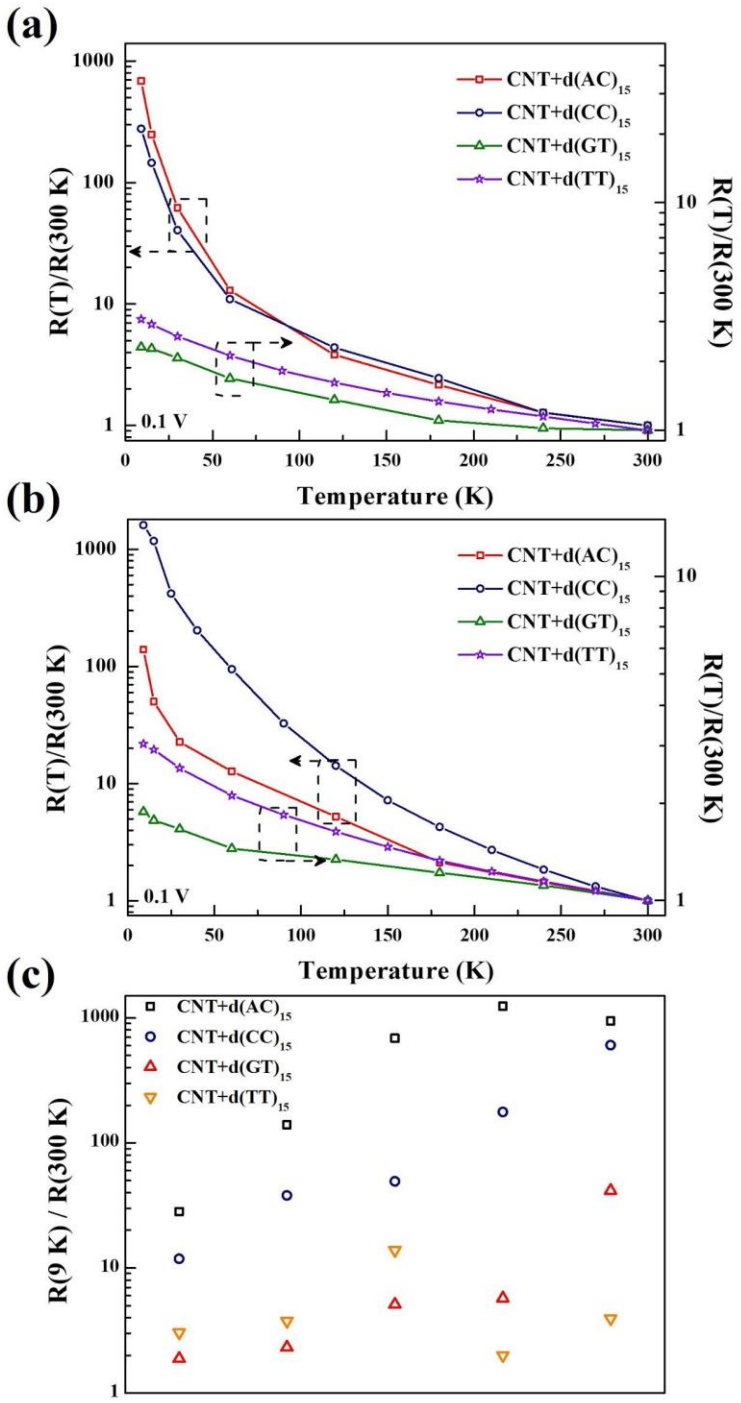

Figure S4. (a), (b) Temperature-dependence of resistance for different functionalizations from *two different sets of samples*. The differences are most significant in the low temperature range (< 50K). (c) Distribution of R(9K)/R(300K) values for different functionalizations measured on different samples.

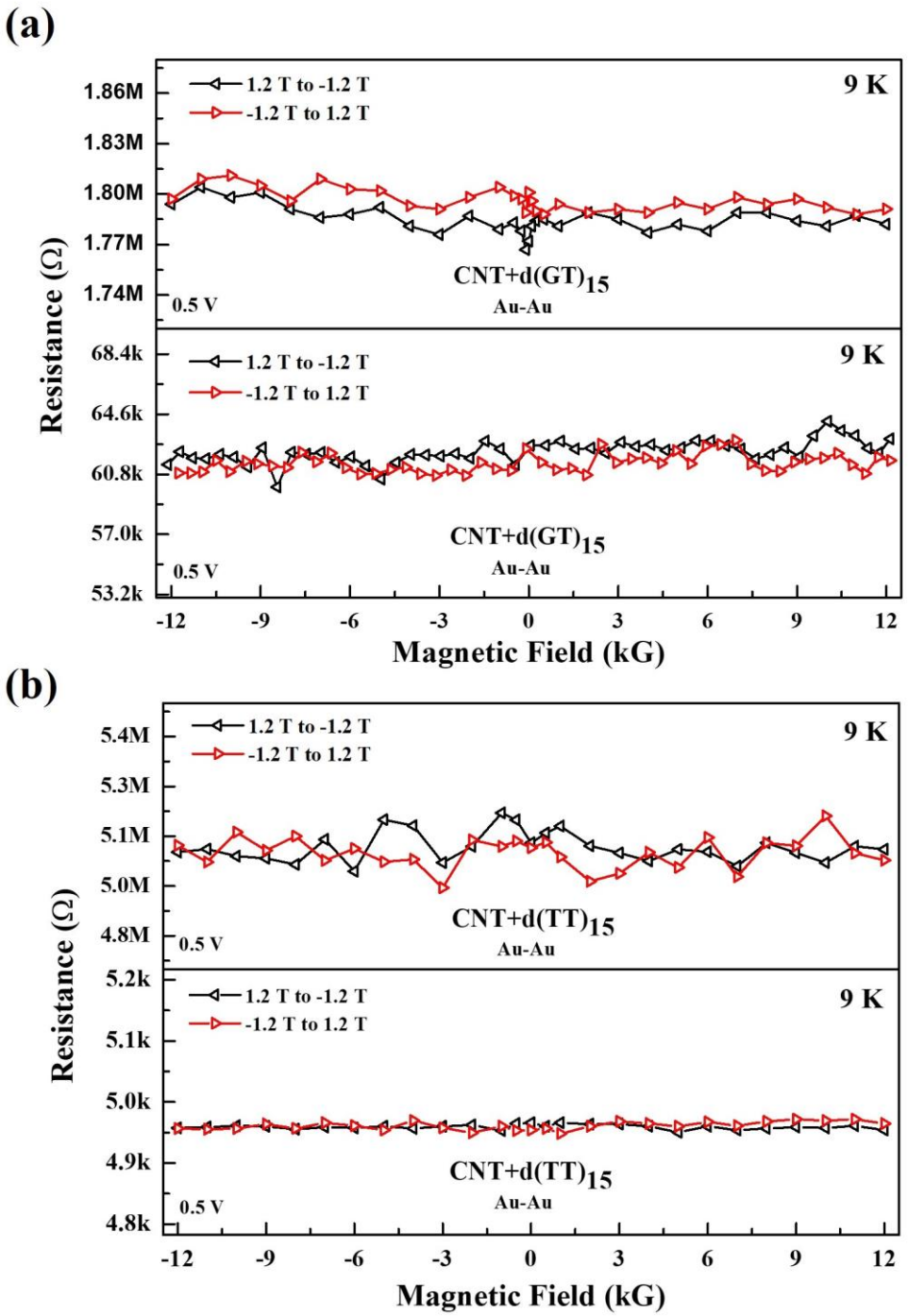

Figure S5. *Absence* of any background negative MR in case of $d(GT)_{15}$ and $d(TT)_{15}$ functionalized CNTs ("strong coupling"). Data from multiple samples have been shown.

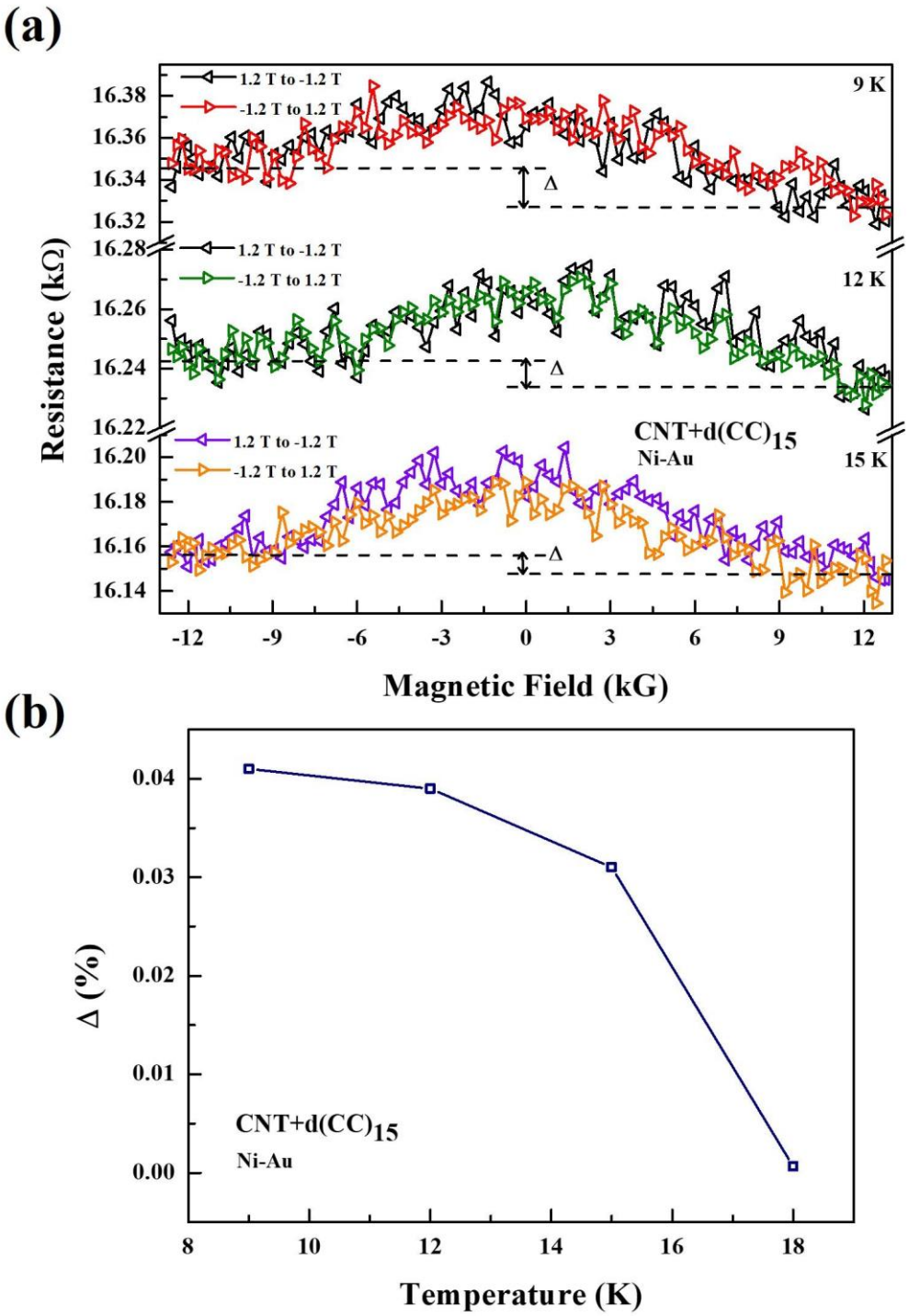

Figure S6. *Asymmetric* MR of $d(CC)_{15}$ wrapped tubes with Ni-Au contacts. The asymmetry (Δ) disappears gradually at higher temperatures.

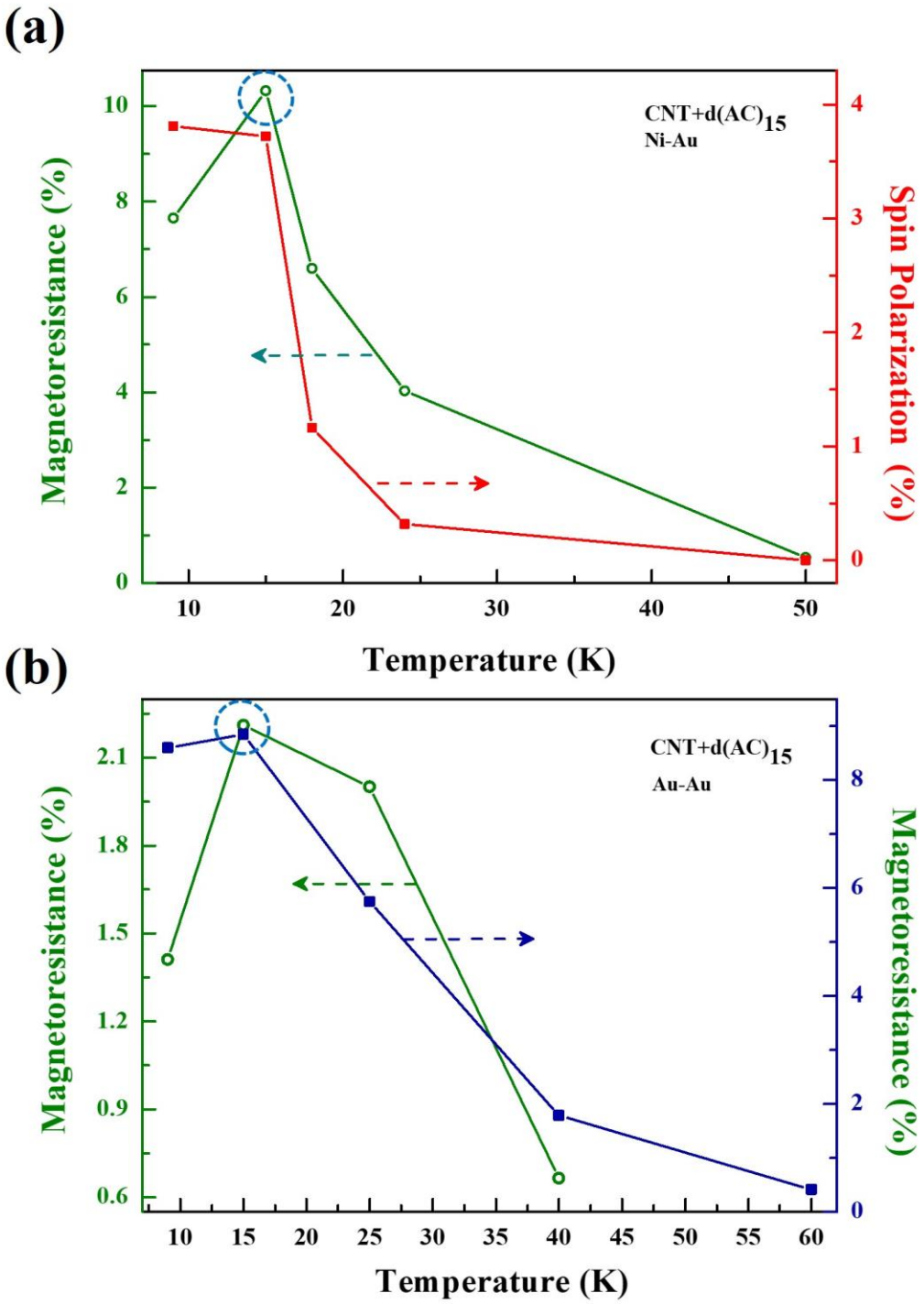

Figure S7. Additional data from *three* different sets of samples showing temperature dependence of MR. (a) Measurement performed on *one* sample using Ni-Au contacts. Both non-monotonic background MR and CISS-induced asymmetric MR (and hence spin polarization) were observed. (b) Measurement performed using Au-Au contacts on *two* different samples. Only non-monotonic background MR was observed. The dashed circle indicates the peak in the non-monotonic (background) MR vs *T* curves.

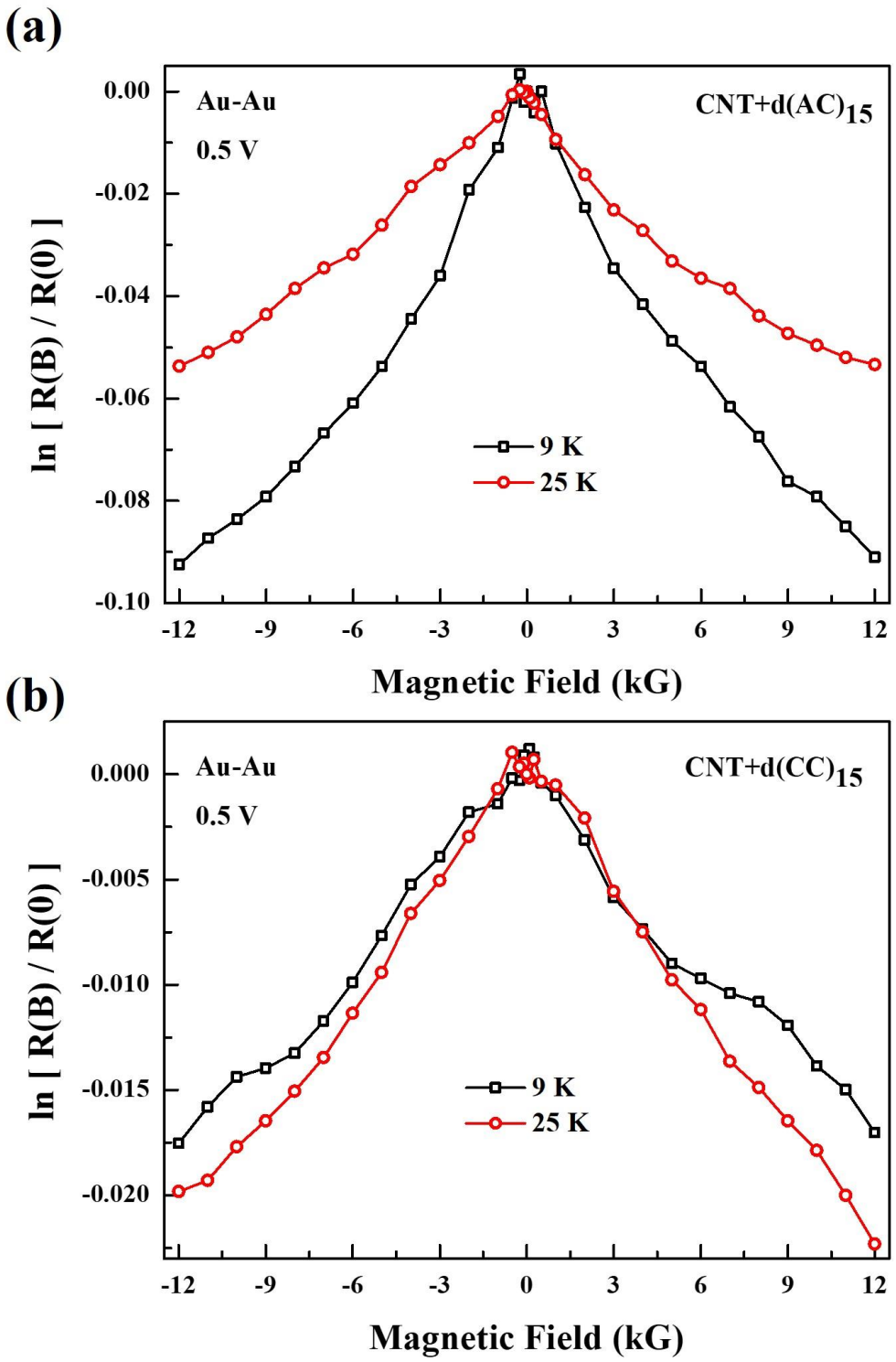

Figure S8. Plot of ln ($R(B)/R(0)$) vs. B for $d(AC)_{15}$ and $d(CC)_{15}$ wrapped CNTs. Absence of a linear fit in the measured field range indicates that the "forward hopping" model described in the main paper is not the dominant transport mechanism.